Supplementary information

Photothermal steam reforming of methane over silica-supported nickel catalysts with temperature gradients

Wirya Sarwana,[a,b] Daichi Takami,[a] Akira Yamamoto,[a,c]* and Hisao Yoshida[a,c,]

[a] Graduate School of Human and Environmental Studies, Kyoto University, Kyoto 606-8501, Japan

[b] Department of Mechanical Engineering, Sumbawa University of Technology, Olat Maras, Sumbawa, West Nusa Tenggara, 84371, Indonesia

[c] Elements Strategy Initiative for Catalysts and Batteries (ESICB), Kyoto University, Kyoto 615-8245, Japan

*Corresponding author: yamamoto.akira.2a@kyoto-u.ac.jp

Contents

Fig. S9. XRD patterns of the Ni-Car samples before and after the PTSRM reaction for 30 h.

Fig. S10. Cyclic reaction tests on the Ni-Car sample in the PTSRM reaction.

Fig. S11. Production rates of H_2, CO_2, and CH_4, and CO conversion of the thermal WGS reaction over the Ni/SiO_2 samples at various temperatures.

Fig. S12. Production rates of CH_4 and CO_2, and CO conversion of the thermal CO hydrogenation reaction over the Ni/SiO_2 samples at various temperatures.

Fig. S13. Production rates of H_2, CO_2, and CH_4, and CO conversion in the thermal WGS and photothermal WGS reactions over Ni-Car at various temperatures.

The crystallite size obtained by the Scherrer equation is volume-weighted average particle size (d_V).[1] The d_V value is different from the number-averaged value for typical TEM analysis when the particle size has distribution. To investigate the consistency between the Ni particle size by TEM and the crystalline size by XRD, we calculated d_V from the particle size distributions by TEM using the following equation[1].

$$d_V = \frac{\sum n_i d_i^4}{\sum n_i d_i^3} \tag{S1}$$

where n_i is the number of the Ni particles with a diameter of d_i.

The order of the d_V values was consistent with the Ni crystalline size by XRD although the absolute values did not coincide. Based on the data, we concluded that the data of Ni particle size by TEM were consistent with the crystalline size by XRD.

Table S1. Volume-weighted particle size (d_V) of the Ni samples

Entry	Sample	d_{XRD} / nm	d_V / nm
1	Ni-Car	18.9	33.1
2	Ni-Ace	11.0	18.1
3	Ni-Nit	24.9	45.5
4	Ni-Lac	43.2	72.3

Table S2. Thermodynamic equilibrium conversion in steam reforming of methane.[a]

T / K	CH_4 conversion (%)	CO selectivity[b] (%)	CO_2 selectivity[c] (%)
573	7.7	0.5	99.5
673	21.7	6.1	93.9
723	32.2	15.2	84.8
773	45.7	31.2	68.8
823	62.1	51.1	48.9
873	79.0	68.2	31.8
973	97.4	83.8	16.2

[a] The calculation was performed at the total pressure of 1 atm using the same concentrations of the reactant gases as the experimental condition. [b] CO selectivity (%) = $[CO]_{eq}$ / ($[CO_2]_{eq}$ + $[CO]_{eq}$) × 100. [c] CO_2 selectivity (%) = $[CO_2]_{eq}$ / ($[CO_2]_{eq}$ + $[CO]_{eq}$) × 100. $[X]_{eq}$ is concentration of X in equblium at the temperatures.
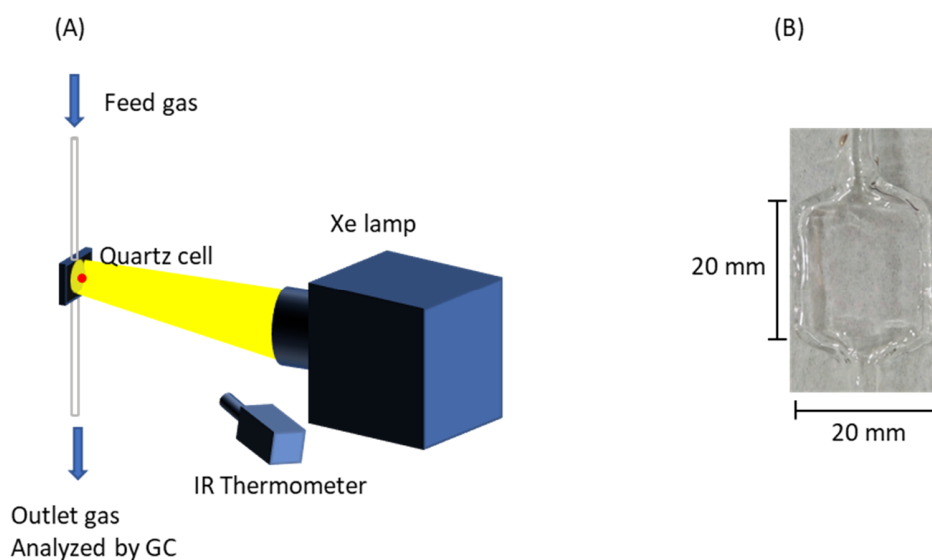
Fig. S1. (A) Experimental set-up of the flow reactor in the photothermal reaction test for PTSRM and (B) digital photograph of the reactor.
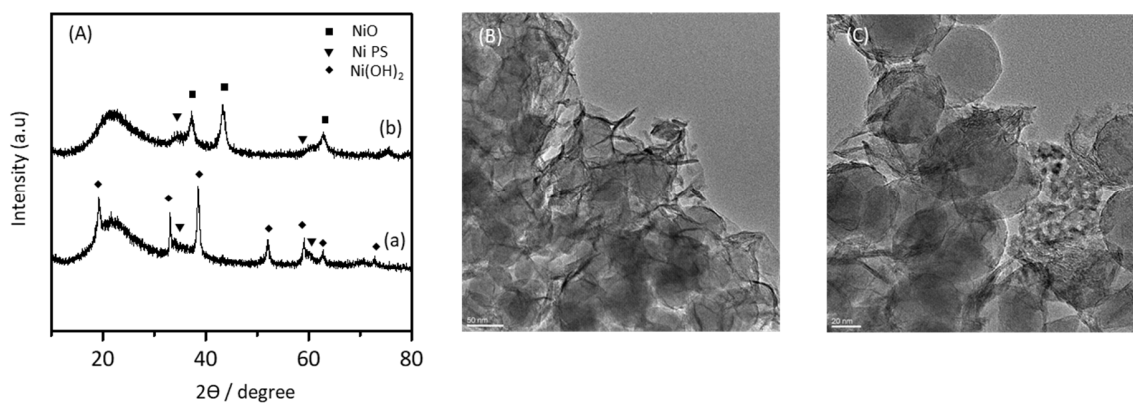
Fig. S2. (A) XRD patterns of the Ni-Car sample after (a) impregnation and (b) calcination at 723 K for 2 hours and TEM images of the Ni-Car sample after (B) impregnation and (C) calcination at 723 K for 2 hours.
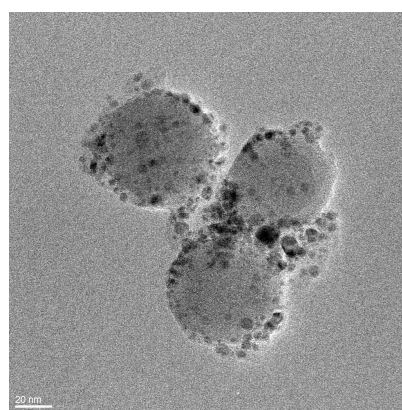
Fig. S3. TEM image of the Ni-Car sample after the reduction treatment in a high magnification.
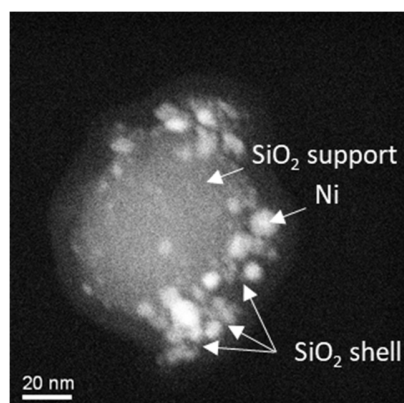
Fig. S4. STEM image of the Ni-Car sample after the reduction treatment.
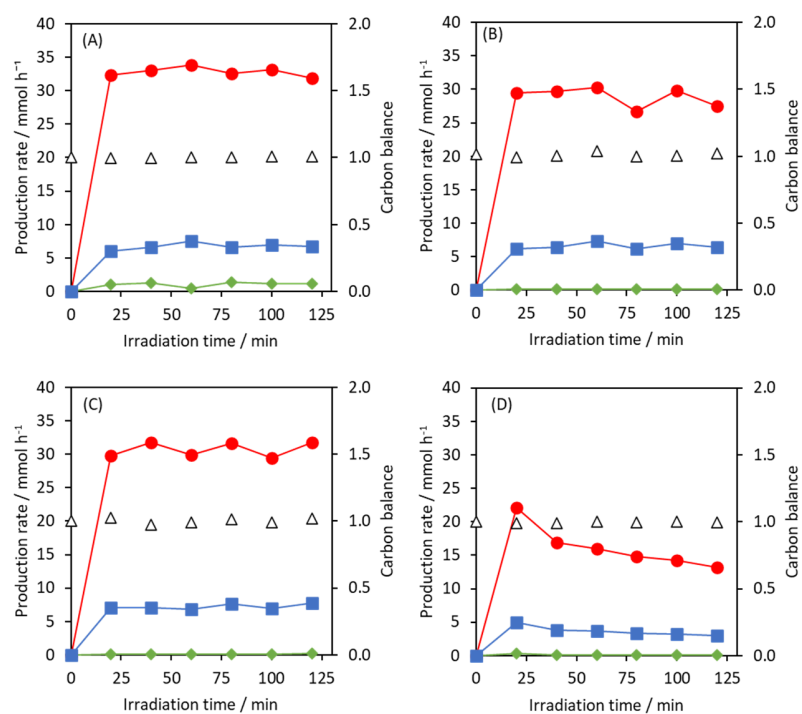
Fig. S5. Time course of the production rates of H_2 (circles), CO_2 (squares), and CO (diamonds) and carbon balance (triangles) in PTSRM. (A): Ni-Car, (B): Ni-Ace, (C): Ni-Nit, and (D): Ni-Lac. Reaction conditions; catalyst weight: 0.5 g, the total gas flow rate: 100 ml min^{-1}, reactant gas concentrations: 8%CH$_4$/12%H$_2$O/6%N$_2$/Ar(balance), light power: 23.8 W, wavelength of light: $\lambda >$ 420 nm.

The TG-DTA measurement was carried out to investigate the coke formation on the spent Ni/SiO_2 catalysts. The measurement was performed under an air atmosphere, and the heating rate was 10 K min^{-1} from room temperature to 1273 K. As shown in Fig. S6, no clear weight loss and exothermic peak due to the oxidation of carbon was recorded in all the Ni/SiO_2 samples used in the PTSRM reaction test in Fig. S5. Separately, the Ni-Lac reduced sample was mixed with 10 wt% of carbon active, and the TG-DTA measurement was performed as a reference. The weight loss (~10%) was observed at around 800–900 K due to the oxidation of carbon. These results indicate that an observable amount of coke was not formed during the PTSRM reaction.
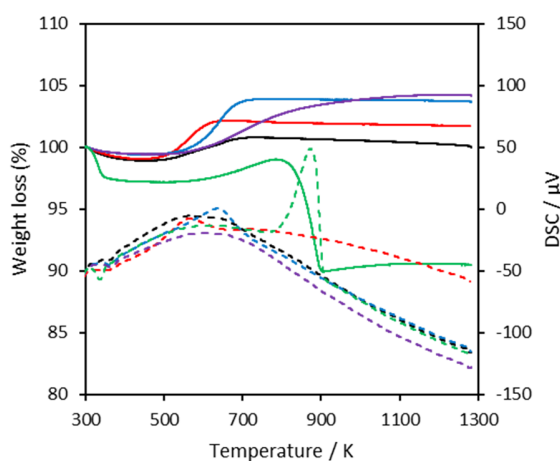
Fig. S6. TG (solid lines) and DTA (dash lines) profiles of the various Ni/SiO_2 samples after the PTSRM reaction for 120 min. Ni-Car: black, Ni-Ace: red, Ni-Nit: blue, and Ni-Lac: violet. Green: reduced Ni-Lac sample mixed with the 10 wt% active carbon as a comparison.
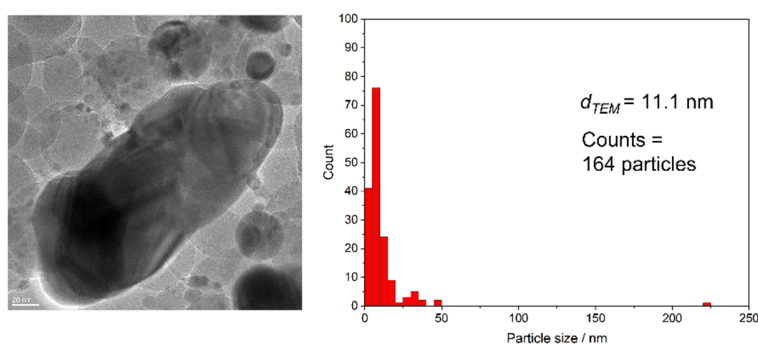
Fig. S7. TEM image and particle size distribution of the Ni-Lac sample after the PTSRM reaction for 120 min.
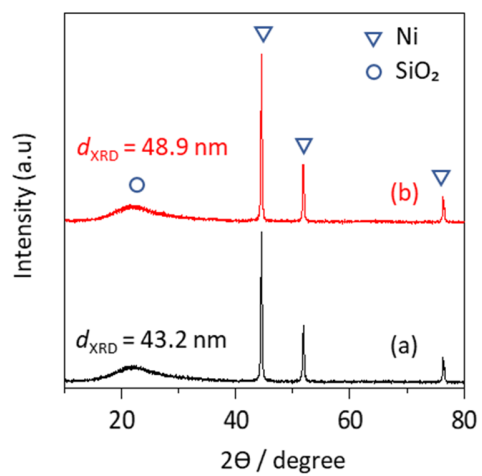
Fig. S8. XRD patterns of the Ni-Lac samples (a) before and (b) after the PTSRM reaction for 120 min.
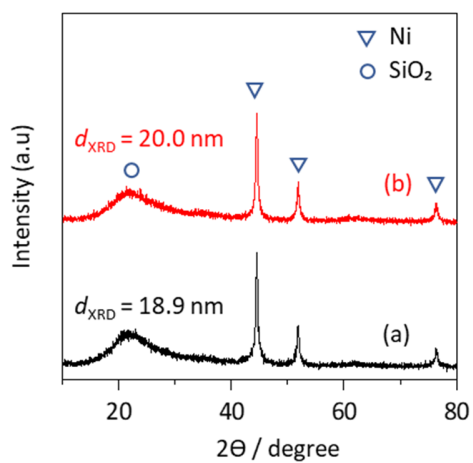
Fig. S9. XRD patterns of the Ni-Car samples (a) before and (b) after the PTSRM reaction for 30 h.
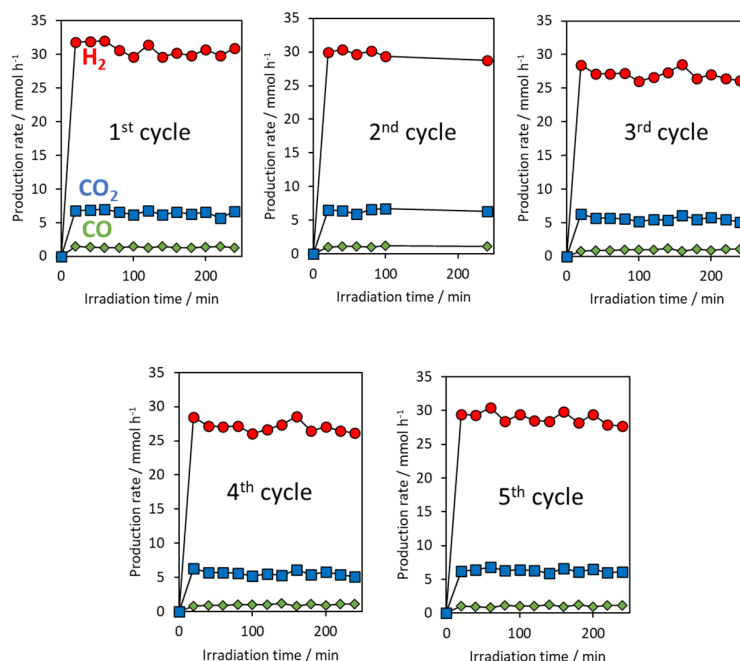
Fig. S10. Cyclic reaction tests of the Ni-Car sample in PTSRM reaction. The reaction conditions were the same as those of Fig. 4.

The activity tests of WGS and CO hydrogenation.

Catalytic activity tests for thermal WGS (CO + $H_2O \rightarrow CO_2$ + H_2, Eq. 2) and CO hydrogenation (CO + $3H_2 \rightarrow$ CH_4 + H_2O, reverse reaction of Eq. 1) were performed by conventional heating using the same experimental conditions as in the cases of the TSRM reaction except for the reactant gas. For WGS and CO hydrogenation, the reactant gases were 5%CO/12%H_2O/10%N_2/Ar(balance) and 5%CO/15%H_2/5%N_2/Ar(balance), respectively, and the total flow rate was fixed to be 100 ml min^{-1}. After the hydrogen pretreatment at 873 K, the reactant gas was introduced to the reactor (the catalyst amount: 0.05 g) and the reaction temperature was increased from 473 K to 773 K. The outlet gas was analyzed 1 h after the objective temperatures were obtained.

The results of the catalytic activity test of WGS were shown in Fig. S11. At 473 K, tiny products were observed over all the Ni samples, and formation rates of H_2 and CO_2 drastically increased over 573 K (Fig. S11A and B). In all catalysts, the formation rates of H_2 and CO_2 were almost the same, which indicates that the WGS reaction proceeded according to the chemical stoichiometry (Eq. 2). Note that tiny amounts of CH_4 were observed possibly due to the reaction of CO or CO_2 with H_2 (methanation of CO or CO_2). The conversion of CO was plotted against the reaction temperature, and it almost reached the equilibrium conversion at 573 K in the Ni-Car sample (Fig. S11D). Overall, the catalytic activity for the WGS reaction was higher than the other samples.
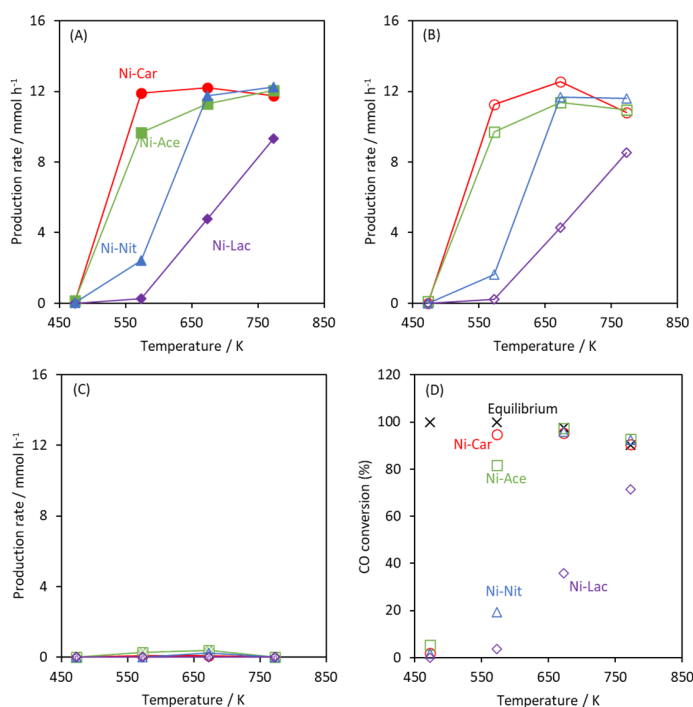
Fig. S11. Production rates of H_2 (A), CO_2 (B), and CH_4 (C), and CO conversion (D) of the thermal WGS reaction over the Ni/SiO_2 samples at various temperatures. Reaction conditions; catalyst weight: 0.05 g, the total gas flow rate: 100 ml min^{-1}, reactant gas concentrations: 5%CO/15%H_2/5%N_2/Ar(balance).

The results of the catalytic activity test of CO hydrogenation were shown in Fig. S12. Compared to the Ni-Ace and Ni-Nit samples, the Ni-Car sample showed lower catalytic activity at the low temperatures of 473 and 573 K (Fig. S12A and B), which clearly indicates that the catalytic performance to consume CO in Ni-Car is lower than Ni-Ace and Ni-Nit by CO hydrogenation in this temperature range. Note that the Ni-Lac sample showed lower CO hydrogenation activity than Ni-Car, but it has also a lower activity for PTSRM, which would result in no CO production on Ni-Lac in PTSRM.

In the Ni samples prepared by the conventional impregnation method (*i.e.*, Ni-Ace, Ni-Nit, Ni-Lac), the catalytic activity in the WGS reaction and CO hydrogenation decreased at 573 K in the following order: Ni-Ace > Ni-Nit > Ni-Lac. This order was the same as the order of the dispersion (Table 1), which indicates that the number of surface-active Ni sites strongly affect the catalytic activity at this temperature. Contrary, Ni-Car did not follow the tendency. As shown in the TEM images, the Ni-Car sample has Ni particles partially encapsulated by SiO_2 (Fig. S3 and S4), which implies that the shell structure has an effect on the catalytic performances of WGS and CO hydrogenation.
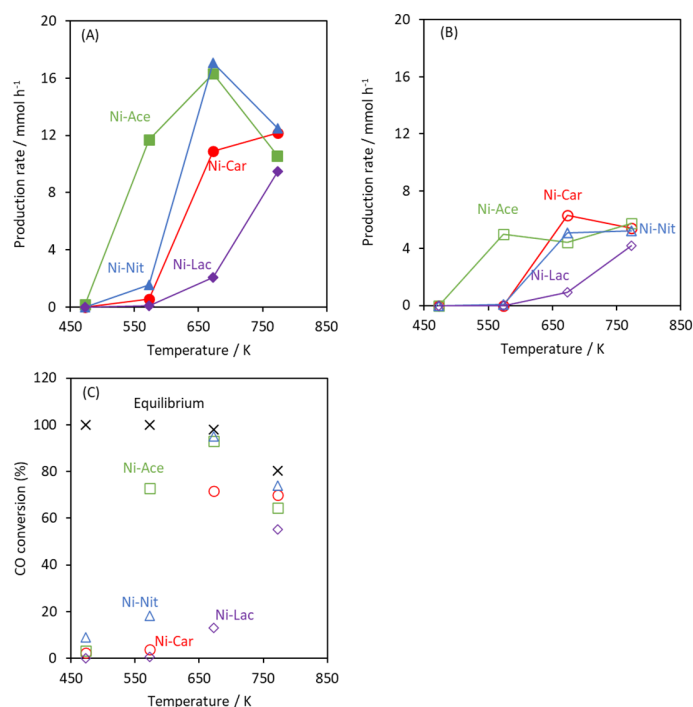
Fig. S12. Production rates of CH_4 (A) and CO_2 (B) and CO conversion (C) of the thermal CO hydrogenation reaction over the Ni/SiO_2 samples at various temperatures. Reaction conditions; catalyst weight: 0.05 g, the total gas flow rate: 100 ml min^{-1}, reactant gas concentrations: 5%CO/15%H_2/5%N_2/Ar(balance).

Comparison of photothermal WGS and thermal WGS

To confirm that the WGS reaction proceeds under photothermal conditions, we performed photothermal WGS on Ni-Car by irradiating at various light intensities (6.6–16 W, spot size: 2 cm) and compared it with the results in the thermal WGS reaction (Fig. S13). Before the activity tests, we performed H_2 reduction pretreatment at 873 K for Ni-Car as in the cases of the PTSRM and thermal WGS reactions. After flowing the reactant gas (5%CO/12%H_2O/10%N_2/Ar(balance), total flow rate: 100 ml min^{-1}), the light power was increased from 6.6 to 16 W to control the maximum surface temperature ($T_{max,f}$) from 573 K to 773 K. The outlet gas was analyzed 1 hour after the objective temperatures were obtained. At 573 K, the catalytic activity and CO conversion in photothermal WGS were much lower than in thermal WGS (Fig. S13) possibly due to the lower temperature zone in the catalyst bed due to the temperature gradient. In contrast, the activity of Ni-Car in photothermal WGS increased drastically over 673 K (Fig. S13A), and at 773 K, the CO conversion became higher than those in the equilibrium and thermal WGS (Fig. S13B). This might be due to the low-temperature zone downstream because the WGS reaction is more favorable at the lower temperatures in the thermodynamics.

11
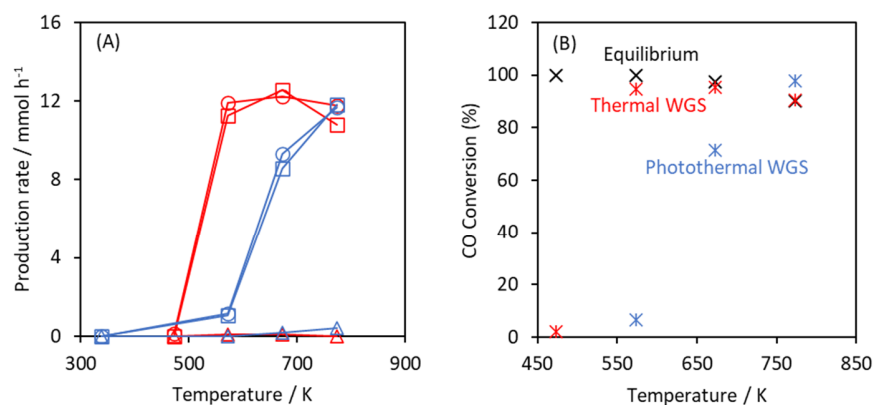
Fig. S13. (A) Production rates of H_2 (open circle), CO_2 (open square), and CH_4 (open triangle), and (B) CO conversion in the thermal WGS (red) and photothermal WGS (blue) reactions over Ni-Car at various temperatures. Reaction conditions; catalyst weight: 0.05 g (thermal WGS) or 0.5 g (photothermal WGS), the total gas flow rate: 100 ml min^{-1}, reactant gas concentrations: 5%CO/12%H_2O/10%N_2/Ar(balance).

References

[1]   R. J. Matyi, L. H. Schwartz and J. B. Butt, *Catal. Rev.*, 1987, **29**, 41–99.